Downloaded from jnm.snmjournals.org by on March 11, 2017. For personal use only.

^{18}F-Labeled Bombesin Analog for Specific and Effective Targeting of Prostate Tumors Expressing Gastrin-Releasing Peptide Receptors

Michael Honer[1], Linjing Mu[1], Timo Stellfeld[2], Keith Graham[2], Miljen Martic[1], Cindy R. Fischer[1], Lutz Lehmann[2], Pius A. Schubiger[1], Simon M. Ametamey[1], Ludger Dinkelborg[2], Ananth Srinivasan[2], and Sandra Borkowski[2]

[1]Department of Chemistry and Applied Biosciences, Center for Radiopharmaceutical Sciences of ETH, PSI, and USZ, Zurich, Switzerland; and [2]Global Drug Discovery, Bayer Healthcare AG, Berlin, Germany

Bombesin is a peptide exhibiting high affinity for the gastrin-releasing peptide receptor (GRPr), which is highly overexpressed on prostate cancer cells. In the present study, we developed an ^{18}F-labeled bombesin analog, ^{18}F-BAY 86-4367, which is currently being clinically tested for use in PET of prostate cancer. **Methods:** In vitro pharmacologic studies were performed to characterize the nonradioactive (^{19}F) standard of the bombesin analog for binding affinity and selectivity for GRPr. The stability of ^{18}F-BAY 86-4367 was determined in murine and human plasma. In vivo, the tumor-targeting potential and pharmacokinetic profile of the ^{18}F tracer were analyzed with biodistribution experiments and PET studies of prostate tumor–bearing mice. **Results:** The nonradioactive (^{19}F) standard of the bombesin analog showed subnanomolar and GRPr-selective binding affinity. The stability of the tracer in murine and human plasma was found to be high. In 2 prostate cancer xenograft models (PC-3 and LNCaP), ^{18}F-BAY 86-4367 showed more specific and effective GRPr-based targeting in vivo than the benchmark radiotracers ^{18}F-fluoroethylcholine and ^{18}F-FDG. In addition, rapid tumor targeting and fast renal excretion (~70%) and hepatobiliary excretion (~10%) were identified in both xenograft models. Furthermore, PET studies provided clear and specific visualization of PC-3 tumors in mice. **Conclusion:** Favorable preclinical data showing specific and effective tumor targeting by ^{18}F-BAY 86-4367 suggest that a clinical trial be undertaken to test its diagnostic utility in PET for prostate carcinoma patients.

Key Words: bombesin; GRPr; PC-3; LNCaP; PET; choline

J Nucl Med 2011; 52:270–278
DOI: 10.2967/jnumed.110.081620

Prostate cancer is the most common nonskin cancer among men in most Western populations, and it is the second leading cause of cancer death in men in the United States (*1*). Advances in the imaging of prostate cancer may help to achieve earlier and more accurate diagnosis and treatment (*2*).

The most widely used PET tracer, ^{18}F-FDG, does not play a prominent role in the diagnosis and staging of prostate cancer, apparently because the use of glucose by prostate carcinoma cells is not enhanced significantly compared with that of normal cells (*3*). Compiled data on staging or restaging for 244 prostate cancer patients suggested an overall sensitivity of only 57% on a per-patient basis. Other PET tracers, such as ^{18}F- or ^{11}C-choline, ^{11}C-acetate, and ^{18}F-fluorothymidine, have shown promise for prostate cancer imaging (*4*). PET/CT with ^{11}C- or ^{18}F-choline is currently considered to be the standard diagnostic imaging tool for the clinical assessment of recurrent prostate cancer in Europe. However, like ^{18}F-FDG, ^{11}C- or ^{18}F-choline is not specific for cancer cells; thus, using this tracer to distinguish benign from malign prostatic tissue is difficult.

The overexpression of the gastrin-releasing peptide receptor (GRPr), also called bombesin receptor subtype 2, on prostate cancer cells provides a potential target for the specific diagnosis and therapy of prostate cancer (*5–7*). Several analogs of the natural GRPr ligand bombesin, a 14-amino-acid neuropeptide, have been labeled with various radionuclides for the diagnosis and treatment of GPRr-positive tumors in recent years (*8–12*). Potent ^{99m}Tc-based (demobesin-1) and ^{111}In-based (RM-1) bombesin analogs that were designed for GRPr-based targeting and tested in the PC-3 xenograft model showed high absolute tumor uptake in animals (*13,14*). Few publications have reported on ^{18}F labeling of bombesin peptides (*15–19*). Our previous study indicated that the negatively charged bombesin derivative 3-cyano-4-^{18}F-fluoro-benzoyl-Ala(SO_3H)-Ava-Gln-Trp-Ala-Val-NMeGly-His-Sta-Leu-NH_2 had much higher prostate tumor uptake than the corresponding positively charged analog (3-cyano-4-^{18}F-fluoro-benzoyl-Arg-Ava-Gln-Trp-Ala-Val-NMeGly-His-Sta-Leu-NH_2) (*20*). Increasing the hydrophilicity as well as the overall charge of the bombesin analog may lead to derivatives with improved sensitivity, specificity, and pharmacokinetics for the optimal targeting of GRPr-positive tumors. Therefore, 1 more L-cysteic acid [Ala(SO_3H)] moiety was inserted in the linker of the

Received Jul. 23, 2010; revision accepted Oct. 26, 2010.
For correspondence or reprints contact: Simon M. Ametamey, Center for Radiopharmaceutical Sciences of ETH, PSI, and USZ, ETH Hönggerberg D-CHAB IPW HCI H427, Wolfgang-Pauli-Strasse 10, CH-8093 Zurich, Switzerland.
E-mail: simon.ametamey@pharma.ethz.ch
COPYRIGHT © 2011 by the Society of Nuclear Medicine, Inc.

Downloaded from jnm.snmjournals.org by on March 11, 2017. For personal use only.

previously mentioned negatively charged bombesin peptide. Here we report on the ^{18}F radiolabeling of this bombesin analog, BAY 86-4367, and a detailed preclinical evaluation of ^{18}F-BAY 86-4367 as a GRPr-selective and metabolically stable imaging agent for prostate cancer.

MATERIALS AND METHODS

General

9-Fluorenylmethoxy carbonyl (Fmoc)-amino acids were purchased from IRIS Biotech, except for Fmoc-statine and Fmoc-Ala(SO_3Na)-OH, which were purchased from NeoMPS (now PolyPeptide Group). Peptide syntheses were performed with rink amide resin (0.68 mmol/g) in accordance with the standard Fmoc strategy. All amino acid residues were, if not further specified, L-amino acid residues. Statine (Sta) denotes (3*S*,4*S*)-4-amino-3-hydroxy-6-methylheptanoic acid, Ala(SO_3H) denotes L-cysteic acid, and Ava denotes 5-aminopentanoic acid. High-performance liquid chromatography (HPLC) analyses were performed with an ACE C18 column (50 × 4.6 mm, 3 μm). Analytic HPLC chromatograms were obtained by use of an Agilent 1100 system equipped with multi-UV-wavelength and Raytest Gabi Star detectors and Gina Star software. Semipreparative HPLC purifications were performed with a semipreparative ACE C18 column (250 × 10 mm, 5 μm). A Merck-Hitachi L6200A system equipped with Knauer variable-wavelength and Eberline radiation detectors was used for semipreparative HPLC. A reversed-phase radio–thin-layer chromatography plate (aluminum sheets, silica gel, RP-$^{18}F_{254}$; Macherey-Nagel) was also used to analyze the ^{18}F-labeled product with 10 mM K_2HPO_4 in water-acetonitrile (3:7) as the mobile phase.

Solid-Phase Peptide Synthesis

Peptide synthesis was performed with Fmoc–rink amide–linker-functionalized polystyrene resin as previously described (*16*). The peptide chain was elongated in cycles of Fmoc deprotection followed by coupling of the subsequent Fmoc-amino acid. Eleven cycles were performed with Fmoc-protected and, if necessary, side chain–protected building blocks of the amino acids, in the following order: leucine (Fmoc-Leu-OH), statine (Fmoc-Sta-OH), histidine (Fmoc-His(Trt)-OH), *N*-methyl-glycine (Fmoc-NMeGly-OH), valine (Fmoc-Val-OH), tryptophan (Fmoc-Trp(Boc)-OH), glutamine (Fmoc-Gln(Trt)-OH), 5-aminopentanoic acid (Fmoc-Ava-OH), and cysteic acid monosodium salt (Fmoc-Ala(SO_3Na)-OH). The Fmoc group of the terminal amino acid was removed to obtain the key intermediate, which was used in the final coupling steps to obtain the precursor (**1a**) as well as the reference standard, the ^{19}F-bombesin analog (**1b**). (4-Carboxy-2-cyanophenyl)-trimethylammonium trifluoromethanesulfonate and 3-cyano-4-fluoro-benzoic acid were used as building blocks for this purpose.

The crude peptide precursor was dried under reduced pressure and purified by preparative HPLC with a Luna C18 column (5 μm; Phenomenex), a mobile phase of acetonitrile (plus 0.1% trifluoroacetic acid [TFA]) and water (plus 0.1% TFA), and a gradient of 5%–30% acetonitrile (20 min). UV peak data were collected and reanalyzed by ultra-performance liquid chromatography–mass spectrometry. Fractions containing the correct mass with a purity of greater than 95% were collected and lyophilized to yield the crystalline product. Starting with 350 μmol of resin, we obtained 112 mg of the product (19% overall yield).

The crude peptide reference standard was purified in a similar procedure by preparative HPLC with a Luna C18 column (5 μm), a mobile phase of acetonitrile (plus 0.1% TFA) and water (plus 0.1% TFA), and a gradient of 5%–40% acetonitrile (20 min). Starting with 100 μmol of resin, we obtained 60 mg of the product (39% overall yield) with a purity of greater than 95%.

Radiochemistry

No-carrier-added ^{18}F-fluoride was produced via the ^{18}O(p,n)^{18}F nuclear reaction by irradiation of enriched ^{18}O-water. ^{18}F-fluoride was immobilized on an anion-exchange cartridge (QMA Light; Waters) and eluted with a solution of Kryptofix K_{222} (5 mg; Merck KGaA) and Cs_2CO_3 (2.3 mg) in acetonitrile (1.5 mL) and water (0.5 mL). The fluoride was dried by azeotropic distillation of acetonitrile at 110°C under vacuum with a stream of nitrogen. The azeotropic drying process was repeated 3 times with 1 mL of acetonitrile each time.

To the dried ^{18}F-fluoride complex (typically 20 GBq), the precursor bombesin peptide (**1a**) was added. To find optimal radiolabeling conditions, we used various solvents (*N,N*-dimethylformamide and dimethyl sulfoxide [DMSO]), reaction temperatures (70°C–100°C), and reaction times (5–20 min), and aliquots of the reaction mixture under the various reaction conditions were analyzed by analytic HPLC. The identity of the tracer (^{18}F-BAY 86-4367) was confirmed by coinjection of the authentic standard (**1b**) into the same analytic HPLC system ACE C18 column (50 × 4.6 mm, 3 μm). The elution conditions were as follows: 10 mM K_2HPO_4 in water (solvent A) and 10 mM K_2HPO_4 in water-acetonitrile (3:7) (solvent B); 0 min, 5% B; 0–7.0 min, 5%–95% B; 7.0–7.1 min, 95%–100% B; 7.1–8.8 min, 100% B; and 8.8–9.0 min, 100%–5% B; and a flow rate of 2 mL/min. The reaction mixture was diluted with water (4 mL) and injected into a semipreparative HPLC ACE column; the conditions were as follows: 0.1% TFA in water (solvent A) and 0.1% TFA in acetonitrile-water (9:1) (solvent B); isocratic elution with 23% solvent B; and a flow rate of 4 mL/min. The product (typically 2 GBq) was collected.

^{18}F-FDG and ^{18}F-fluoroethylcholine (^{18}F-FCH) were purchased from University Clinic Charité and Eckert & Ziegler, respectively.

Determination of Distribution Coefficient

The distribution coefficient was determined by the shake flask method (*21*). In brief, the peptide was dissolved in a mixture of phosphate buffer (600 μL, pH 7.4) and *n*-octanol (600 μL) at 20°C. The sample was equilibrated by 4 min of shaking followed by centrifugation. The concentration of the peptide in each phase was measured by HPLC-UV absorption. The distribution coefficient was calculated as the log ratio of the UV peak areas at 254 nm in the organic and aqueous phases.

In Vitro Characterization

Displacement Assays. The binding affinities of the nonradioactive ^{19}F-bombesin peptide for human GRPr and neuromedin B receptor were determined by use of a scintillation proximity assay (SPA) with transfected cellular membranes (RBHBS2 M and RBHBS1 M; PerkinElmer) and either ^{125}I-Tyr^4-bombesin or the universal ligand [D-^{125}I-Tyr^6,βAla^{11},Phe^{13},Nle^{14}]bombesin (each at 81.4 TBq/mmol; PerkinElmer) as a radioligand. The membranes and agglutinin-coupled SPA beads (type A; polyvinyltoluene (PVT)- and polyethyleneimine-treated wheat germ; Amersham Bioscience) were mixed in incubation buffer (50 mM Tris-HCl [pH 7.2], 5 mM $MgCl_2$, 1 mM ethylene glycol tetraacetic acid, protease inhibitor [1 tablet per 50 mL; Roche Diagnostics GmbH], and 0.3% polyethyleneimine) to produce final protein concentrations of 20 μg/mL

Downloaded from jnm.snmjournals.org by on March 11, 2017. For personal use only.

(RBHBS2 M) and 28 μg/mL (RBHBS1 M) and a final concentration of PVT-SPA beads of 8 mg/mL. The radioligands were diluted to either 0.2 nM (^{125}I-Tyr^4-bombesin) or 0.5 nM ([D-^{125}I-Tyr^6,βAla^{11},Phe^{13},Nle^{14}]bombesin) in incubation buffer. The inhibitor used for displacement was either nonradioactive ^{19}F-bombesin (**1b**) or neuromedin B (Sigma). The test compounds were dissolved in DMSO to produce 1 mM stock solutions and further diluted in incubation buffer to 2 pM–1,000 nM. Nonspecific binding was determined with an excess (>1,000-fold) of either Tyr^4-bombesin or [D-Tyr^6,βAla^{11},Phe^{13},Nle^{14}]bombesin (Sigma).

The SPA was performed in quadruplicate as follows. First, 10 μL of a test compound was placed in white 384-well plates (Lumitrac 200; Greiner). Next, 20 μL of the GRPr–PVT-SPA bead mixture and 20 μL of the ligand solution were added. After 120 min of incubation at room temperature, 50 μL of incubation buffer were added; the plate was sealed and centrifuged for 10 min at 520*g* and room temperature. Signals were quantified with a Top Count (PerkinElmer) for 60 s of integration per well. Nonspecific binding was subtracted from total binding to yield specific binding at each concentration. The 50% inhibitory concentration (IC_{50}) and the inhibition constant (K_i) were calculated by nonlinear regression with GraFit 5 data analysis software (Erithacus Software Ltd.).

Scatchard Assays. For saturation binding analysis, human PC-3 prostate carcinoma cells (American Type Culture Collection) at confluence were placed in 48-well plates (8×10^4 cells per well). Cells were incubated in triplicate with increasing concentrations of the ^{18}F-labeled bombesin analog (0.05 nM–100 nM) in binding buffer (50 mM *N*-(2-hydroxyethyl)piperazine-*N*′-(2-ethanesulfonic acid), 1 mM ethylenediaminetetraacetic acid, 5 mM $MgCl_2$, and 0.1% bovine serum albumin [pH 7.4] in Dulbecco modified Eagle medium with GlutaMAX I [Invitrogen]) to produce a total volume of 200 μL. The concentration range was selected on the basis of the IC_{50} of the nonradioactive peptide (see earlier description). Nonspecific binding was determined in the presence of 1 μM Tyr^4-bombesin for each radioligand concentration. After incubation at room temperature for 1 h, cells were washed twice with cold phosphate-buffered saline (PBS) (plus 0.1% bovine serum albumin) and solubilized with 300 μL of 0.25% trypsin-ethylenediaminetetraacetic acid solution (incubation for 20 min at 37°C) and then washed with 1 mL of PBS. Radioactivity was measured with a γ-counter (Wizard; PerkinElmer). Saturation binding data were evaluated with KELL Radlig software (Biosoft). Three independent experiments were performed, and the dissociation constant was calculated by use of the Scatchard transformation.

In Vitro Stability Studies. The stability of the radiolabeled bombesin analog was investigated in mouse and human plasma at various incubation times (0–120 min) and 37°C. PBS was used as a control. After incubation, plasma proteins were precipitated with acetonitrile and centrifuged for 10 min at 13,000*g* and 4°C. The PBS control was diluted with the same volume of acetonitrile. The supernatants and the PBS control were analyzed by analytic HPLC.

In Vivo Characterization

In Vivo Stability Studies. All animal experiments were undertaken in compliance with the current version of the Swiss and German law concerning animal protection and welfare. Male NMRI nude mice were injected intravenously with approximately 25 MBq of the ^{18}F-bombesin derivative. Animals were sacrificed at 1, 3, 5, 10, and 15 min after injection, and blood and urine were collected. Aliquots of plasma and urine were mixed with acetonitrile for protein precipitation. The samples were centrifuged at 5,000*g* (Megafuge R; Heraeus), and the supernatants were analyzed by radio-HPLC with a Luna C18 column (0.1% TFA in water [solvent A] and 0.1% TFA in acetonitrile-water [9:1] [solvent B]).

Biodistribution Studies. Biodistribution experiments were performed with male NMRI nude mice bearing subcutaneous PC-3 or LNCaP tumors next to the right shoulder. For induction of the xenografts, tumor cells (2×10^6 cells per mouse) were injected subcutaneously and allowed to grow for 4 wk. The sizes of the PC-3 tumors ranged from 40 to 450 mg, and the sizes of the LNCaP tumors ranged from 90 to 700 mg. Animals were injected intravenously in the tail vein with 45–238 kBq of the bombesin tracer (100 μL). Radioactive doses of the comparative tracers ^{18}F-FDG and ^{18}F-FCH were 180–225 kBq/100 μL per animal. Animals were sacrificed at various times (0.5–4 h; $n = 3$ for each time point). Organs and tissues of interest were collected and weighed. The amount of radioactivity was determined with the γ-counter to calculate uptake as the percentage injected dose per gram of tissue (%ID/g). In addition, 3 mice that received a coinjection of 100 μg of Tyr^4-bombesin and the radiolabeled compound were sacrificed at 1 h after injection to determine nonspecific tissue uptake.

PET Studies. PET of PC-3 tumor–bearing mice was performed with the 16-module variant of the dedicated small-animal PET quad-HIDAC tomograph (Oxford Positron Systems) (*22*). Animals were injected intravenously with 9–20 MBq (<1 nmol) of the radioligand and scanned in a whole-body configuration from 60 to 105 min after injection. Animals were anesthetized with isoflurane and monitored as reported previously (*22*). Two animals received a coinjection of 100 μg of bombesin (1 mg/mL), and 2 animals received a corresponding volume of vehicle. After termination of the PET scan, animals were sacrificed at 107 min after injection by decapitation for tissue sampling. PET data were reconstructed in a single 45-min time frame and normalized to the injected dose per gram of body weight.

RESULTS

Chemistry and Radiochemistry

The bombesin peptide analog was synthesized by solid-phase peptide synthesis in accordance with standard Fmoc strategy. Coupling of the resin-bound peptide with 3-cyano-4-fluoro-benzoic acid and 3-cyano-4-trimethylamino-benzoic acid yielded the corresponding nonradioactive (^{19}F) peptide standard (**1b**) and precursor (**1a**) for ^{18}F labeling, respectively. The ^{19}F-bombesin peptide served as a surrogate for the ^{18}F-bombesin peptide in the determination of binding affinity and as a reference standard for radio-HPLC analysis. Figure 1 shows the sequences of **1a** and **1b** and the structures of the nonnatural amino acid derivatives. The synthesized bombesin precursor and reference standard were characterized by mass spectrometry:

3-cyano-4-trimethylammonium-benzoyl-Ala(SO_3H)-Ala(SO_3H)-Ava-Gln-Trp-Ala-Val-NMeGly-His-Sta-Leu-NH_2-trifluoroacetate salt (**1a**, 112 mg, 19%)—*m/z* $[M]^+$ calculated: 1,567.7, found: 1,567.5

Downloaded from jnm.snmjournals.org by on March 11, 2017. For personal use only.

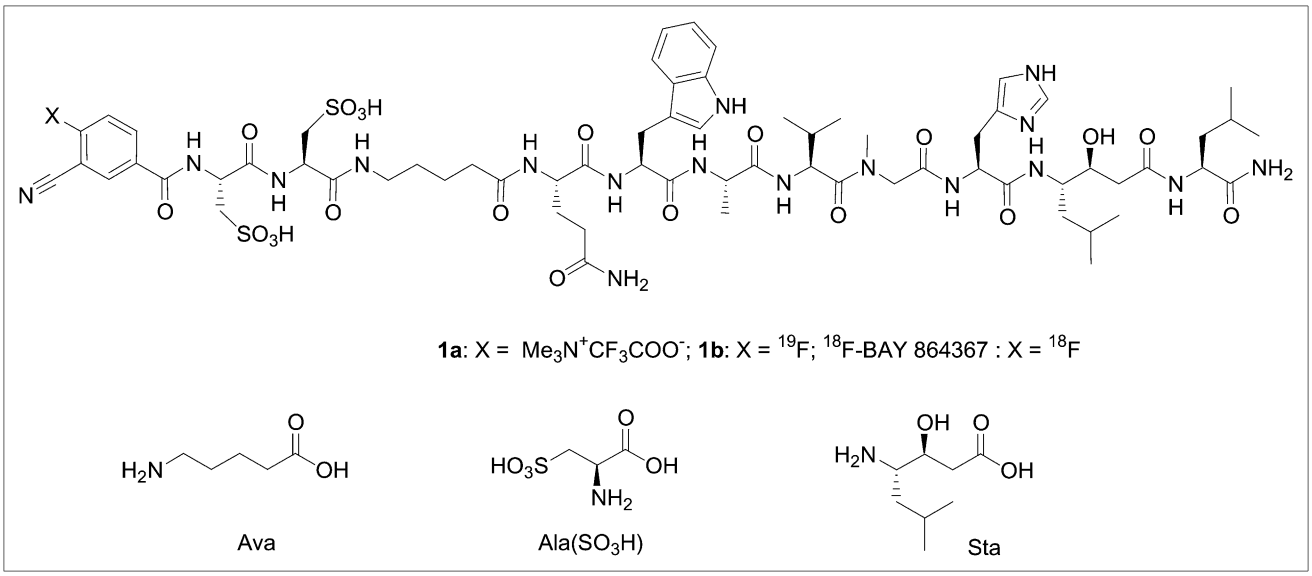


FIGURE 1. Peptide sequences and structures of nonnatural amino acids. **1a** = precursor; **1b** = reference compound or ^{18}F-BAY 86-4367.

3-cyano-4-fluoro-benzoyl-Ala(SO_3H)-Ala(SO_3H)-Ava-Gln-Trp-Ala-Val-NMeGly-His-Sta-Leu-NH2 (**1b**, 60 mg, 39%)—*m/z* $[M+H]^+$ calculated: 1,528.6, found: 1,528.9.

Direct 1-step ^{18}F labeling via aromatic nucleophilic substitution of ^{18}F for $^+N(CH_3)_3$—developed previously in our laboratories—was successfully applied to the bombesin peptide analog (*19*). Using DMSO as the solvent resulted in a higher level of ^{18}F incorporation than using *N,N*-dimethylformamide at all of the tested reaction temperatures. The required reaction temperature and time for sufficient ^{18}F labeling efficiency were either 80°C or 90°C and 5 min, respectively. For all of the in vitro and in vivo studies, ^{18}F labeling of the peptide was performed with 2 mg of precursor in 150 μL of DMSO in the presence of a $Cs^{18}F$-Kryptofix K_{222} complex. The reaction mixture was heated at 90°C for 10 min; after semipreparative HPLC purification, the product fraction was collected. The collected product was diluted with water (18 mL), immobilized on the cartridge, and washed with water (2 × 10 mL), and then the radioactive bombesin derivative was eluted with ethanol (1.5 mL). The solvent was evaporated at 80°C under vacuum with a stream of nitrogen and subsequently dissolved in saline-water. The decay-corrected radiochemical yield of the isolated product was approximately 15%, and the radiochemical purity was always greater than 95%. The specific activity after formulation was up to 170 GBq/μmol.

Distribution Coefficient

The distribution coefficient of the nonradioactive ^{19}F-bombesin derivative was determined by the shake flask method and HPLC-UV absorption. This coefficient was found to be lower than −3.9 at pH 7.4, indicating a highly hydrophilic peptide.

In Vitro Characterization

Displacement and Scatchard Assays. The affinity of the bombesin peptide analog for GRPr was in the subnanomolar range, with an IC_{50} (mean ± SD) of 0.94 ± 0.19 nM and a K_i of 0.13 ± 0.05 nM (n = 3) (Fig. 2). Saturation binding assays revealed 40,000–60,000 binding sites per PC-3 cell and less than 10,000 binding sites per LNCaP cell. The selectivity of ^{18}F-BAY 86-4367 for GRPr was demonstrated in a displacement assay with neuromedin B receptor–transfected cell membranes and [D-^{125}I-Tyr^6,βAla^{11},Phe^{13},Nle^{14}]bombesin as a universal bombesin receptor ligand. The natural ligand

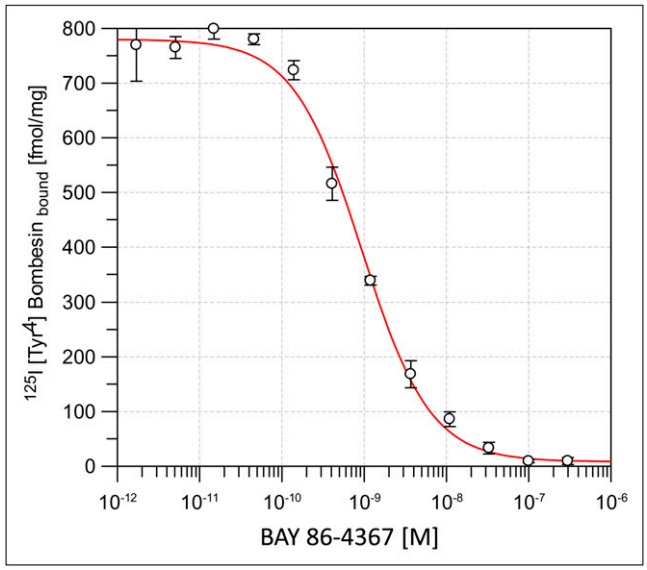


FIGURE 2. Competitive binding of ^{18}F-BAY 86-4367 and radioligand ^{125}I-Tyr^4-bombesin in SPA with membranes of GRPr-transfected cells.

Downloaded from jnm.snmjournals.org by on March 11, 2017. For personal use only.

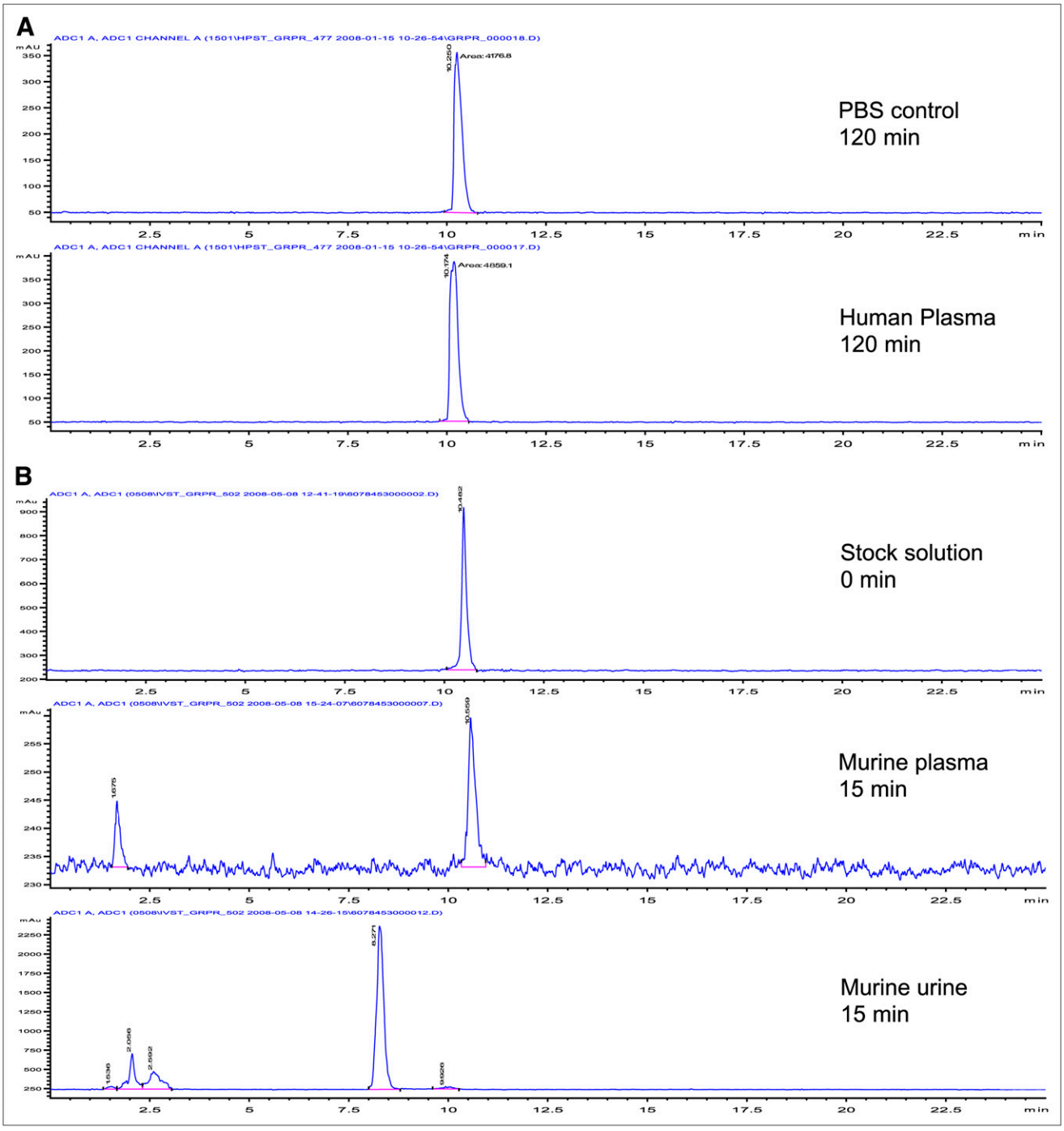


FIGURE 3. (A) In vitro stability of ^{18}F-BAY 86-4367 in human plasma and in PBS. (B) In vivo metabolism of radiolabeled peptide in murine plasma and urine.

neuromedin B had a high affinity for bombesin 3 receptors (IC_{50}, 20.6 nM), but ^{18}F-BAY 86-4367 exhibited no such affinity (IC_{50}, >10,000 nM) (Supplemental Table 1) (supplemental materials are available online only at http://jnm.snmjournals.org).

The binding affinity of ^{18}F-BAY 86-4367 for human PC-3 prostate carcinoma cells was analyzed by saturation binding assays and then Scatchard transformation. Radioligand binding was found to be saturable with a single high-affinity binding site; the dissociation constant was 1.43 ± 0.25 nM (n = 3) (Supplemental Fig. 2). These findings suggest that under the radiolabeling conditions (90°C for 10 min), the affinity of the peptide for GRPr was retained.

Additionally, the antagonistic properties of ^{18}F-BAY 86-4367 were determined with 2 assays—receptor internalization visualized by immunofluorescence microscopy (*23,24*) and cellular calcium mobilization (*25*)—performed in the laboratory of Jean C. Reubi (University of Bern). Bombe-

Downloaded from jnm.snmjournals.org by on March 11, 2017. For personal use only.

sin-induced GRPr internalization in human GRPr–transfected HEK cells and calcium mobilization in PC-3 cells were efficiently antagonized by the nonradioactive bombesin peptide (Supplemental Fig. 3). These findings suggest that the candidate compound behaves as an antagonist for GRPr.

In Vitro Stability. The radiolabeled compound did not show any degradation either in PBS or in mouse or human plasma up to 120 min (Fig. 3A).

In Vivo Characterization

In Vivo Stability. The in vivo stability of ^{18}F-BAY 86-4367 was analyzed in murine plasma and urine by radio-HPLC. At various times after radiotracer injection into nude mice (1–15 min), blood and urine were collected for HPLC analysis. At 15 min after injection, only 1 minor polar radiometabolite could be detected in the plasma (Fig. 3B). A prominent metabolite, more hydrophilic than the parent compound, was already found in the urine after 5 min.

Biodistribution Studies. High PC-3 tumor uptake of the radiotracer was found at 1 h after injection (6.2 %ID/g), and this uptake could be blocked effectively (>80%) by coinjection of nonradioactive bombesin (100 μg per mouse) (Table 1). The tumor-to-blood ratio at 1 h after injection was 19. The GRPr-expressing murine pancreas also showed high uptake of the radiotracer (>40 %ID/g). Other GRPr-positive organs showing natural specific uptake were the adrenal glands, stomach, and intestine. The radioactive peptide showed gallbladder uptake of 30–50 %ID/g even at early times, indicating rapid liver metabolism of parts of the circulating tracer. Subsequent intestinal excretion

TABLE 1
Biodistribution of ^{18}F-BAY 86-4367 in PC-3 Tumor–Bearing Mice at Various Times After Injection and After 60 Minutes of Blocking (n = 3)

	10 min		20 min		30 min		60 min		60-min block (100 μg of nonradioactive bombesin)	
Parameter	Mean	SD	Mean	SD	Mean	SD	Mean	SD	Mean	SD
%ID/g in:										
Spleen	1.03	0.23	0.47	0.14	1.10	0.57	0.83	0.46	3.76	0.67
Liver	4.53	1.42	1.84	0.17	1.81	0.32	0.76	0.05	3.93	0.14
Kidneys	7.44	1.84	2.85	0.25	3.58	0.53	2.19	0.15	2.54	0.36
Lungs	1.98	0.86	0.70	0.10	0.75	0.05	0.43	0.11	115.03	28.24
Bone*	0.75	0.18	0.73	0.07	0.83	0.05	1.58	0.09	1.73	0.44
Heart	0.98	0.36	0.36	0.05	0.32	0.08	0.22	0.02	0.63	0.07
Brain	0.09	0.02	0.04	0.00	0.05	0.01	0.03	0.00	0.06	0.01
Fat	0.75	0.48	0.10	0.01	0.21	0.12	0.09	0.01	0.15	0.02
Thyroid	1.73	0.47	0.53	0.13	0.64	0.14	0.46	0.03	0.73	0.04
Gallbladder	29.92	43.85	49.96	34.24	82.08	35.06	36.33	6.59	10.89	8.70
Muscle	0.47	0.26	0.18	0.03	0.17	0.03	0.17	0.09	0.14	0.00
Tumor	4.66	0.20	4.98	1.18	5.91	1.05	6.19	2.49	1.10	0.44
Skin*	2.06	0.82	0.71	0.11	0.75	0.27	0.38	0.04	0.41	0.02
Blood	2.16	1.00	0.72	0.11	0.70	0.14	0.33	0.03	0.53	0.05
Tail	4.67	1.37	2.99	1.43	2.24	0.60	0.74	0.11	4.41	2.92
Stomach	3.01	1.03	3.90	1.86	3.41	0.57	2.70	0.73	0.33	0.07
Prostate	1.47	0.56	0.40	0.07	0.59	0.42	0.28	0.04	0.27	0.21
Intestine	4.09	0.75	4.88	0.63	4.73	1.06	4.98	0.90	2.81	1.00
Pancreas	39.30	3.73	40.69	5.34	45.90	2.57	36.84	4.29	1.36	0.46
Adrenal glands	6.09	0.68	4.37	1.02	3.28	1.17	2.83	0.36	0.75	0.33
Additional %ID:										
Recovery	98.37	1.06	87.61	2.06	96.28	5.00	97.96	7.68	94.63	1.94
Organs	55.59	5.11	37.98	3.12	46.02	1.33	36.77	1.41	59.43	2.55
Carcass	23.20	3.67	15.03	4.34	15.32	4.55	8.71	1.53	9.40	0.94
Urine	19.53	9.17	34.57	8.86	34.91	10.69	56.19	4.25	25.94	2.23
Feces			0.00	0.00	0.00	0.01	0.58	1.01	0.01	0.00
Ratio of tumor to:										
Liver	1.11	0.36	2.73	0.82	3.38	1.06	7.99	2.90	0.28	0.12
Kidneys	0.66	0.20	1.75	0.41	1.68	0.40	2.78	0.99	0.46	0.26
Blood	2.47	1.02	7.00	1.82	8.86	2.98	18.55	6.40	2.15	1.10
Muscle	11.98	5.49	29.74	12.74	35.13	2.09	49.55	33.01	7.65	3.15
Bone	6.46	1.46	6.91	2.12	7.14	1.16	3.97	1.73	0.72	0.49

*Tissue aliquots only.

Downloaded from jnm.snmjournals.org by on March 11, 2017. For personal use only.

resulted in 10 %ID in the feces at 4 h after injection. In parallel, rapid urinary excretion of radioactivity was found, with 50 %ID already in the urine after 1 h. Tumor-to-tissue ratios at 1 h after injection were predominantly much greater than 1. The tumor uptake of ^{18}F-BAY 86-4367 was also quantified for LNCaP tumors, which showed less than half of the activity concentration of PC-3 tumors, with 2.3 %ID/g at 1 h after injection because of a lower level of GRPr expression (Table 2). All other organ uptake values were comparable to the biodistribution values obtained in PC-3 tumor–bearing animals.

In the next set of biodistribution experiments, the uptake of ^{18}F-BAY 86-4367 was compared with that of ^{18}F-FCH and ^{18}F-FDG at 1 h after injection in prostate tumor–bearing mice. ^{18}F-BAY 86-4367 showed the most favorable distribution in both prostate tumor models, with high tumor uptake, low nontarget uptake, and rapid excretion (Table 2). Urinary excretion was lowest with ^{18}F-FCH. Tumor-to-tissue ratios in PC-3 tumor–bearing mice at 1 h after injection were markedly higher for the radioactive peptide tracer than for ^{18}F-FCH and ^{18}F-FDG in the same tumor model.

PET of PC-3 Tumor–Bearing Mice. Nude mice bearing subcutaneous PC-3 tumor xenografts next to the right shoulder were scanned from 60 to 105 min after injection in a dedicated small-animal PET system under both baseline and blocking conditions (Fig. 4). The tumors were clearly imaged under baseline conditions, whereas no tumor was visualized under blocking conditions. As expected from the ex vivo biodistribution studies, the highest activity concentrations in the in vivo PET studies were identified in the urinary bladder, the gallbladder, and the intestine. Clear visualization of the GRPr-positive pancreas by PET was not possible because of the proximity of the pancreas to the bowel. Postmortem tissue sampling of the mice after PET (at 107 min after injection) confirmed the data obtained in the biodistribution studies. The absolute radioactivity uptake values in the GRPr-rich tissues were 4.7 %ID/g for the tumor and 15.6 %ID/g for the pancreas. The specificities of uptake for the tumor and the pancreas were 82% and 96%, respectively.

TABLE 2
Biodistribution of ^{18}F-BAY 86-4367 (^{18}F-BN), ^{18}F-FCH, and ^{18}F-FDG in PC-3 and LNCaP Tumor–Bearing Mice at 60 Minutes (n = 3)

	Tumor-bearing mice									
	PC-3						LNCaP			
	^{18}F-BN		^{18}F-FCH		^{18}F-FDG		^{18}F-BN		^{18}F-FCH	
Parameter	Mean	SD	Mean	SD	Mean	SD	Mean	SD	Mean	SD
%ID/g in:										
Spleen	0.83	0.46	3.02	0.99	1.30	0.09	0.40	0.03	4.07	0.51
Liver	0.76	0.05	7.20	0.29	0.77	0.15	0.69	0.01	10.89	2.75
Kidneys	2.19	0.15	14.47	3.27	0.89	0.13	1.69	0.11	12.53	0.72
Lungs	0.43	0.11	8.95	1.44	3.02	0.25	0.47	0.05	6.81	1.05
Bone	1.58	0.09	2.27	0.43	2.45	0.36	1.42	0.14	2.02	0.47
Heart	0.22	0.02	6.48	0.45	46.53	12.09	0.23	0.05	6.03	0.17
Brain	0.03	0.00	0.56	0.03	4.69	0.63	0.03	0.00	0.48	0.09
Fat	0.09	0.01	0.30	0.11	2.02	1.42	0.59	0.62	0.27	0.01
Thyroid	0.46	0.03	4.18	0.42	6.33	0.47	0.57	0.12	4.20	1.17
Gallbladder	36.33	6.59	2.68	1.48			21.75	30.81	2.09	0.73
Muscle	0.17	0.09	1.84	0.31	3.86	0.91	0.13	0.03	1.41	0.30
Tumor	6.19	2.49	1.02	0.08	2.44	0.21	2.28	0.19	0.87	0.32
Skin	0.38	0.04	1.92	0.14	1.69	0.24	0.54	0.23	1.96	0.06
Blood	0.33	0.03	0.64	0.05	0.36	0.02	0.38	0.04	0.72	0.06
Tail	0.74	0.11	3.34	1.22	1.23	0.07	0.89	0.04	4.73	2.40
Stomach	2.70	0.73	4.10	0.28	2.79	1.19	2.76	0.30	4.43	0.30
Prostate	0.28	0.04	2.45	0.73			0.46	0.19	1.86	0.11
Intestine	4.98	0.90	2.35	0.20	1.47	0.08	5.08	0.13	2.38	0.34
Pancreas	36.84	4.29	5.28	0.70	2.08	0.48	35.61	2.75	4.26	0.45
Adrenal glands	2.83	0.36	6.70	1.51	4.16	0.72	2.48	1.23	3.58	0.49
%ID excreted in:										
Urine	56.19	4.25	9.78	2.36	17.91	4.19	45.25	12.42	6.28	2.31
Feces	0.58	1.01	0.77	1.03	0.24	0.29	0.10	0.15	0.01	0.01
Ratio of tumor to:										
Liver	7.99	2.90	0.14	0.01	3.23	0.48	3.31	0.25	0.08	0.01
Kidneys	2.78	0.99	0.07	0.02	2.80	0.53	1.35	0.19	0.07	0.02
Blood	18.55	6.40	1.60	0.04	6.67	0.27	6.03	0.95	1.23	0.47
Muscle	49.55	33.01	0.56	0.05	0.65	0.14	19.22	6.85	0.61	0.14
Bone	3.97	1.73	0.46	0.07	1.01	0.15	1.62	0.23	0.43	0.08

Downloaded from jnm.snmjournals.org by on March 11, 2017. For personal use only.

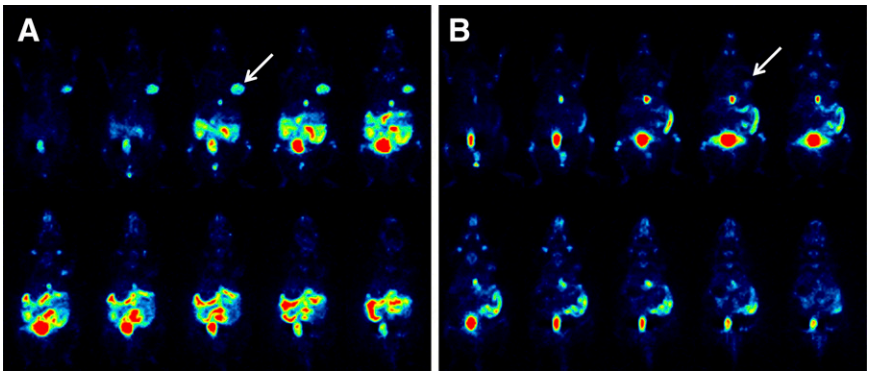


FIGURE 4. Series of horizontal whole-body slices (ventral to dorsal) from 2 nude mice bearing subcutaneous PC-3 tumor xenografts next to right shoulder (arrows). Mice were injected with ^{18}F-BAY 86-4367 and scanned from 60 to 105 min after injection under baseline (A) and blocking (B) conditions. Image data were normalized to injected dose per gram of body weight.

DISCUSSION

Numerous bombesin analogs have been radiolabeled with a variety of radioactive isotopes for the detection and therapy of GRPr-expressing neoplasms (*8–12,26–29*). Tetraamine-functionalized ^{99m}Tc-bombesin analogs with favorable in vivo profiles were reported by Nock et al. (*28*). Parry et al. also reported that ^{64}Cu-DOTA-bombesin peptides exhibited tumor uptake and good imaging characteristics (*30*). Our laboratories have focused on labeling peptides for PET of both breast cancer and prostate cancer with ^{18}F because this nuclide has ideal characteristics for peptide receptor imaging studies.

The precursor and reference standard were prepared by solid-phase peptide synthesis in optimal yields. The distribution coefficient of the nonradioactive ^{19}F-bombesin derivative (**1b**) was lower than −3.9. The direct labeling of peptides with ^{18}F in a single step was recently described by various groups (*19,31–33*). Schirrmacher et al. reported the direct radiolabeling of an organosilicon-modified peptide in an isotope exchange reaction (*32*). Several 1-step approaches for the facile ^{18}F labeling of peptides have been developed in our laboratories (*19,31,33*). In the present study, ^{18}F labeling of BAY 86-4367 was achieved in a single step via aromatic nucleophilic substitution. ^{18}F-BAY 86-4367 was obtained in a good radiochemical yield and with excellent radiochemical purity after HPLC purification.

The affinity of ^{18}F-BAY 86-4367 for GRPr was high—in the subnanomolar range—whereas the affinity of ^{18}F-BAY 86-4367 for the other 2 bombesin receptor subtypes, neuromedin B and bombesin 3 receptors, was negligible. Tumor accumulation of ^{18}F-BAY 86-4367 was investigated in PC-3 (androgen-independent human prostate cancer with a high level of GRPr expression) and LNCaP (androgen-dependent human prostate cancer with a lower level of GRPr expression than PC-3) tumor–bearing mice. High and persistent tracer uptake in PC-3 tumors and GRPr-expressing murine organs (pancreas, stomach, intestine, and adrenal glands) was identified. LNCaP tumors showed 50% less tracer uptake than PC-3 tumors because of a lower level of GRPr expression, as reported previously. Compared with ^{18}F-FCH and ^{18}F-FDG, the tracer candidate displayed the highest tumor-to-tissue ratios in PC-3 tumor–bearing mice. In line with the results of the biodistribution studies, PET images showed highly specific GRPr targeting of the radiotracer in PC-3 tumor–bearing mice, as demonstrated by effective blocking with nonradioactive Tyr^4-bombesin.

Recent preclinical studies demonstrated that GRPr antagonists may be preferable to agonists for tumor targeting, yielding high tumor uptake and long tumor washout (*23,34*). Our data indicated that ^{18}F-BAY 86-4367 behaves as an antagonist for GRPr, making this peptide promising for further evaluation in a clinical trial.

On the basis of the aforementioned in vivo results, ^{18}F-BAY 86-4367 has favorable pharmacokinetics, with rapid tumor targeting, rapid blood clearance, and fast and predominantly renal excretion (~70%). This advantageous pattern of elimination, in combination with high affinity and specificity, suggest that ^{18}F-BAY 86-4367 may have higher diagnostic accuracy than the standard tools ^{18}F-FDG and ^{18}F-FCH in PET for prostate cancer patients.

CONCLUSION

The favorable preclinical data obtained for ^{18}F-BAY 86-4367 suggest that a clinical trial be undertaken to test its diagnostic utility for prostate carcinoma patients. A clinical proof-of-mechanism microdosing study in healthy volunteers and patients is currently under way to assess the tumor-targeting potential, radiation dosimetry, pharmacokinetics, and metabolism of the tracer candidate in a clinical setting.

ACKNOWLEDGMENTS

We would like to thank Jean C. Reubi and his coworkers for performing the antagonist studies and Claudia Keller, Sabine Baumann, René Zernicke, Ingolf Weber, Volker Stickel, and Melanie Appel for their excellent technical assistance.

Downloaded from jnm.snmjournals.org by on March 11, 2017. For personal use only.

REFERENCES

1. Jemal A, Siegel R, Ward E, Murray T, Xu JQ, Thun MJ. Cancer statistics, 2007. *CA Cancer J Clin.* 2007;57:43–66.
2. Hong H, Zhang Y, Sun JT, Cai WB. Positron emission tomography imaging of prostate cancer. *Amino Acids.* 2010;39:11–27.
3. Jana S, Blaufox MD. Nuclear medicine studies of the prostate, testes, and bladder. *Semin Nucl Med.* 2006;36:51–72.
4. Ravizzini G, Turkbey B, Kurdziel K, Choyke PL. New horizons in prostate cancer imaging. *Eur J Radiol.* 2009;70:212–226.
5. Reile H, Armatis PE, Schally AV. Characterization of high-affinity receptors for bombesin/gastrin releasing peptide on the human prostate-cancer cell-lines Pc-3 and Du-145: internalization of receptor-bound ^{125}I-(Tyr^4) bombesin by tumor-cells. *Prostate.* 1994;25:29–38.
6. Markwalder R, Reubi JC. Gastrin-releasing peptide receptors in the human prostate: relation to neoplastic transformation. *Cancer Res.* 1999;59:1152–1159.
7. Chung DH, Evers BM, Beauchamp RD, et al. Bombesin stimulates growth of human gastrinoma. *Surgery.* 1992;112:1059–1065.
8. Hoffman TJ, Gali H, Smith CJ, et al. Novel series of In-111-labeled bombesin analogs as potential radiopharmaceuticals for specific targeting of gastrin-releasing peptide receptors expressed on human prostate cancer cells. *J Nucl Med.* 2003; 44:823–831.
9. Maecke HR, Hofmann M, Haberkorn U. Ga-68-labeled peptides in tumor imaging. *J Nucl Med.* 2005;46(suppl):172S–178S.
10. Rogers BE, Bigott HM, McCarthy DW, et al. MicroPET imaging of a gastrin-releasing peptide receptor-positive tumor in a mouse model of human prostate cancer using a Cu-64-labeled bombesin analogue. *Bioconjug Chem.* 2003;14: 756–763.
11. Schweinsberg C, Maes V, Brans L, et al. Novel glycated [Tc-99m(CO)$_3$]-labeled bombesin analogues for improved targeting of gastrin-releasing peptide receptor-positive tumors. *Bioconjug Chem.* 2008;19:2432–2439.
12. Schroeder RPJ, van Weerden WM, Bangma C, Krenning EP, de Jong M. Peptide receptor imaging of prostate cancer with radiolabelled bombesin analogues. *Methods.* 2009;48:200–204.
13. Nock B, Nikolopoulou A, Chiotellis E, et al. [Tc-99m]demobesin 1, a novel potent bombesin analogue for GRP receptor-targeted tumour imaging. *Eur J Nucl Med Mol Imaging.* 2003;30:247–258.
14. Mansi R, Wang XJ, Forrer F, et al. Evaluation of a 1,4,7,10-tetraazacyclododecane-1,4,7,10-tetraacetic acid-conjugated bombesin-based radioantagonist for labeling with single-photon emission computed tomography, positron emission tomography, and therapeutic radionuclides. *Clin Cancer Res.* 2009;15:5240–5249.
15. Zhang XZ, Cai WB, Cao F, et al. F-18-labeled bombesin analogs for targeting GRP receptor-expressing prostate cancer. *J Nucl Med.* 2006;47:492–501.
16. Hoehne A, Mu L, Honer M, et al. Synthesis, F-18-labeling, and in vitro and in vivo studies of bombesin peptides modified with silicon-based building blocks. *Bioconjug Chem.* 2008;19:1871–1879.
17. Li ZB, Wu ZH, Chen K, Ryu EK, Chen XY. F-18-labeled BBN-RGD heterodimer for prostate cancer imaging. *J Nucl Med.* 2008;49:453–461.
18. Liu ZF, Yan YJ, Liu SL, Wang F, Chen XY. F-18, Cu-64, and Ga-68 labeled RGD-bombesin heterodimeric peptides for PET imaging of breast cancer. *Bioconjug Chem.* 2009;20:1016–1025.
19. Becaud J, Mu L, Karramkam M, et al. Direct one-step ^{18}F-labeling of peptides via nucleophilic aromatic substitution. *Bioconjug Chem.* 2009;20:2254–2261.
20. Mu L, Honer M, Becaud J, et al. In vitro and in vivo characterization of novel 18F-labeled bombesin analogues for targeting GRPR-positive tumors. *Bioconjug Chem.* 2010;21:1864–1871.
21. Strijckmans VH, Dolle F, Coulon C. Synthesis of a potential M_1 muscarinic agent, ^{76}Br-bromocaramiphen. *J Labelled Comp Radiopharm.* 1996;42:447–456.
22. Honer M, Bruhlmeier M, Missimer J, Schubiger AP, Ametamey SM. Dynamic imaging of striatal D-2 receptors in mice using quad-HIDAC PET. *J Nucl Med.* 2004;45:464–470.
23. Cescato R, Maina T, Nock B, et al. Bombesin receptor antagonists may be preferable to agonists for tumor targeting. *J Nucl Med.* 2008;49:318–326.
24. Cescato R, Schulz S, Waser B, et al. Internalization of sst_2, sst_3, and sst_5 receptors: effects of somatostatin agonists and antagonists. *J Nucl Med.* 2006;47:502–511.
25. Ginj M, Zhang HW, Waser B, et al. Radiolabeled somatostatin receptor antagonists are preferable to agonists for in vivo peptide receptor targeting of tumors. *Proc Natl Acad Sci USA.* 2006;103:16436–16441.
26. Lin KS, Luu A, Baidoo KE, et al. A new high affinity technetium analogue of bombesin containing DTPA as a pharmacokinetic modifier. *Bioconjug Chem.* 2004;15:1416–1423.
27. Chen XY, Park R, Hou YP, et al. microPET and autoradiographic imaging of GRP receptor expression with Cu-64-DOTA-[Lys$_3$]bombesin in human prostate adenocarcinoma xenografts. *J Nucl Med.* 2004;45:1390–1397.
28. Nock BA, Nikolopoulou A, Galanis A, et al. Potent bombesin-like peptides for GRP-receptor targeting of tumors with Tc-99m: a preclinical study. *J Med Chem.* 2005;48:100–110.
29. Gourni E, Paravatou M, Bouziotis P, et al. Evaluation of a series of new Tc-99m-labeled bombesin-like peptides for early cancer detection. *Anticancer Res.* 2006;26:435–438.
30. Parry JJ, Kelly TS, Andrews R, Rogers BE. In vitro and in vivo evaluation of Cu-64-labeled DOTA-linker-bombesin(7-14) analogues containing different amino acid linker moieties. *Bioconjug Chem.* 2007;18:1110–1117.
31. Mu L, Hohne A, Schubiger RA, et al. Silicon-based building blocks for one-step F-18-radiolabeling of peptides for PET imaging. *Angew Chem Int Ed.* 2008; 47:4922–4925.
32. Schirrmacher R, Bradtmoller G, Schirrmacher E, et al. F-18-labeling of peptides by means of an organosilicon-based fluoride acceptor. *Angew Chem Int Ed.* 2006;45:6047–6050.
33. Roehn U, Becaud J, Mu LJ, et al. Nucleophilic ring-opening of activated aziridines: a one-step method for labeling biomolecules with fluorine-18. *J Fluor Chem.* 2009;130:902–912.
34. Abd-Elgaliel WR, Gallazzi F, Garrison JC, et al. Design, synthesis, and biological evaluation of an antagonist-bombesin analogue as a targeting vector. *Bioconjug Chem.* 2008;19:2040–2048.

Downloaded from jnm.snmjournals.org by on March 11, 2017. For personal use only.

JNM The Journal of NUCLEAR MEDICINE

^{18}F-Labeled Bombesin Analog for Specific and Effective Targeting of Prostate Tumors Expressing Gastrin-Releasing Peptide Receptors

Michael Honer, Linjing Mu, Timo Stellfeld, Keith Graham, Miljen Martic, Cindy R. Fischer, Lutz Lehmann, Pius A. Schubiger, Simon M. Ametamey, Ludger Dinkelborg, Ananth Srinivasan and Sandra Borkowski

J Nucl Med. 2011;52:270-278.
Published online: January 13, 2011.
Doi: 10.2967/jnumed.110.081620

This article and updated information are available at:
http://jnm.snmjournals.org/content/52/2/270

Information about reproducing figures, tables, or other portions of this article can be found online at:
http://jnm.snmjournals.org/site/misc/permission.xhtml

Information about subscriptions to JNM can be found at:
http://jnm.snmjournals.org/site/subscriptions/online.xhtml

The Journal of Nuclear Medicine is published monthly.
SNMMI | Society of Nuclear Medicine and Molecular Imaging
1850 Samuel Morse Drive, Reston, VA 20190.
(Print ISSN: 0161-5505, Online ISSN: 2159-662X)

© Copyright 2011 SNMMI; all rights reserved.

SNMMI SOCIETY OF NUCLEAR MEDICINE AND MOLECULAR IMAGING